An attempt to synthesize 2D layered non-Pb halide double perovskite using organic spacer cations

Dhanvin M Koundinya

MS15186

A dissertation submitted for the partial fulfilment of
BS-MS dual degree in Science

Indian Institute of Science Education and Research Mohali
May 2020

Certificate of Examination

This is to certify that the dissertation titled "An attempt to synthesize 2D layered non-Pb halide double perovskite using organic spacer cations" submitted by Mr. Dhanvin M Koundinya (Reg. No. MS15186) for the partial fulfillment of BS-MS dual degree programme of the Institute, has been examined by the thesis committee duly appointed by the Institute. The committee finds the work done by the candidate satisfactory and recommends that the report be accepted.

Dr. Ujjal K. Gautam   Dr. A. R. Choudhury   Dr. Debrina Jana

                                                          (Supervisor)

                                                          Dated: June 15, 2020

Declaration

The work presented in this dissertation has been carried out by me under the guidance of Dr. Debrina Jana at the Indian Institute of Science Education and Research, Mohali.

This work has not been submitted in part or in full for a degree, a diploma, or a fellowship to any other university or institute. Whenever contributions of others are involved, every effort is made to indicate this clearly, with due acknowledgement of collaborative research and discussions. This thesis is a bonafide record of original work done by me and all sources listed within have been detailed in the bibliography.

Dhanvin M Koundinya

(Candidate)

Dated: June 15, 2020

In my capacity as the supervisor of the candidate's project work, I certify that the above statements by the candidate are true to the best of my knowledge.

Dr. Debrina Jana

(Supervisor)

Acknowledgement

Dhanvin M Koundinya

CONTENTS

NOTATIONS

kWh – Kilo Watt per hour

DP – Double Perovskite

Å – Angstrom

2D – 2-Dimension

OIHP – Organic Inorganic Hybrid
Perovskites

NC- Nano-Crystals

PSC – Perovskite Solar Cells

XRD – X-ray Diffraction

TEM – Transmission Electron
Microscopy

HRTEM – High Resolution
Transmission Electron Microscopy

eV – Electron Volt

PL – Photoluminescence

nm – nano-meters

DP - Double Perovskite

HIOP - Hybrid Inorganic Organic Perovskites

p - Holes

n – Electrons

UV- Vis – Ultra Violet - Visible

pH – Power of Hydrogen

A – Absorbance

I_o – Incident Light Intensity

I – Transmitted Light Intensity

ε - Molar Absorption Coefficient

l – Path Length

c – Concentration of Sample

λ – Wavelength

$λ_0$ – Maximum Absorption Wavelength

$\log_{10}$ – log to the base 10

d_{hkl} – Interplanar Spacing

Ɵ - Bragg's Angle

LIST OF ELEMENTS/COMPOUNDS

Ca – Calcium

O – Oxygen

Br – Bromine

Cl – Chlorine

C – Carbon

N – Nitrogen

Cs – Cesium

Ag – Silver

Sb – Antimony

Pb - Lead

Mo – Molybdenum

CTAB – Cetrimonium
bromide

NH_3^+ - Ammonium ion

LIST OF FIGURES

CHAPTER -1 INTRODUCTION

CHAPTER – 2 CHARACTERISATION TECHNIQUES

CHAPTER – 3 SYNTHESIS

LIST OF TABLES

CHAPTER 3 - Synthesis

ABSTRACT

The introduction of double perovskite has lead to develop Lead-free perovskites that have similar properties to that of the predecessors, with nearly the same efficiency. Three-dimensional (3D) hybrid organic−inorganic lead halide perovskites (HOIPs) feature remarkable optoelectronic properties for solar energy conversion but suffer from longstanding issues of environmental stability and lead toxicity. Associated two-dimensional (2D) analogues are garnering increasing interest due to superior chemical stability, structural diversity, and broader property tunability.

Toward lead-free 2D HOIPs, double perovskites (DPs) with mixed-valent dual metals are attractive. Translation of mixed-metal DPs to iodides, with their prospectively lower bandgaps, represents an important target for semiconducting halide perovskites, but has so far proven inaccessible using traditional spacer cations due to either intrinsic instability or formation of competing non-perovskite phases, thus usage of bromides id due to its optical properties which are highly tunable, through varying the layer thickness and increasing the length of the organic spacer. Here are critical measures of ongoing works concentrated on the two-dimensional (2D) perovskite materials due to their special physical and compound properties emerging from the quantum confinement impact. This thesis work characterizes upon the fact of synthesizing $A_2AgSbBr_6$ with different spacer cations, and since many Bi DPs have been synthesized and Sb is isoelectronic to Sb, thus it can also be used for processing DPs. The second chapter helps in understanding the different characterization techniques which were used in the experimentation processes to recognize the formation of certain perovskites. The characterization processes used were Photoluminescence, UV-Vis Spectroscopy and X-Ray Diffraction.

The third chapter of synthesis helps in understanding the production by amount of the certain perovskites using different spacer cations. The fourth chapter helps in the characterization of these attempts to synthesize the hybrid perovskites, followed by the final chapter of future aspects and its outlook.

CHAPTER 1 – INTRODUCTION

1.1. Demand for alternate source of energy

The demand for energy and development of industrialization, the non-renewable fossil fuels have dragged humanization into an energy crisis. The consumption of fossil fuels to produce energy by its combustion causes air pollution and climate change, which have serious international implications from the past decade. Due to these causes, people are finding other alternative renewable sources of power, such as solar energy, wind, hydro-energy to replace the non-renewable sources. These are being greatly developed over the past few years, as shown by the figures for Great Britain electricity generation by renewable during 2003-2016 in Fig. 1.1. Of all the renewable energies, solar power is believed to be the supply of nearly all energy on the earth. It is so abundant that the energy from sunlight hit on the earth in a year is as high as 1.5×1018 kWh, that is quite 100 times the   entire energy   of well-known fuel reserves everywhere the planet. [1] Thus the development of an efficient way to make use of solar power would be highly helpful for fulfilling societal demand. Photovoltaic cells are one way to reap the solar energy.
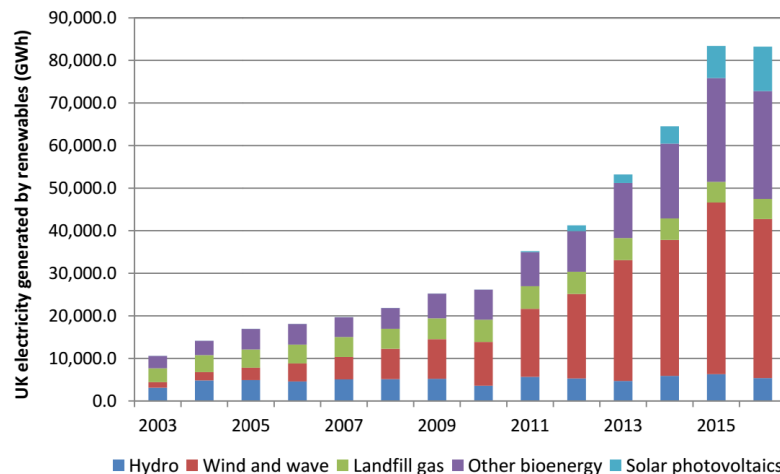
Fig. 1.1 Electricity generation by renewable sources in UK during 2003-2016. Reproducedfrom data provided by National Statistics. [Reproduced from Reference Number : 1]

1.2. Lead-Halide Perovskites

Lead-Halide perovskites are the frontrunners for the third generation in solution based photovoltaic research. Due to its low cost and higher power conversion efficiencies, they are closed to being commercialized. Especially, the prime discovery is the well balanced electron-hole diffusions and gain properties in these materials emerge as a prominent role in discovering structure-function relationship and giving access to potential feedback for material development.[2]

The general structure of a Pb-Halide perovskite can be classified as ABX_3 type perovskite. Here A^+ is a mono-valent cation and $[BX_6]^{4-}$ has a octahedral structure that form the unit cell, where B^{2+} is the Pb^{2+} ion and X^- is the halide. The basic perovskite structure is shown below in Fig 1.2.
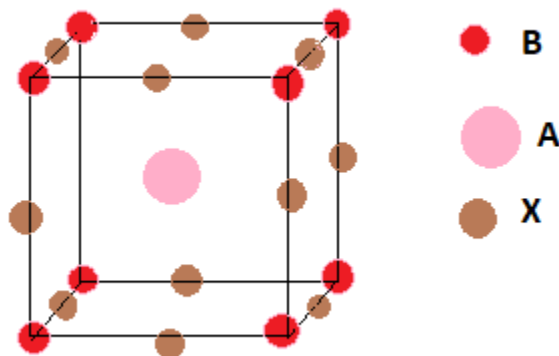
Fig 1.2. ABX_3 perovskite structure where, A represent the mono-valent cation, B the Pb^{2+} and X^- the halide ions. [Reproduced from Reference Number 3]

The advantaged of Pb-Halide based perovskites are mainly attributed to its stability in organic solvents and ease-of-tuning heir band edges. These perovskites are easy to process, low cost and moisture tolerant which bring new breakthrough in Material Chemistry. [4]

One of the main drawback of these Lead-based Halide Perovskite is that it contains Pb which is a harmful chemical to the nature. Even though the production cost is low, the

toxicity caused due to these perovskites make them vulnerable for further production, hence it was necessary to develop an alternative to it.

1.3. What is a Double Perovskite?

Double Perovskites (DP) were created to tackle the problem for replacing Pb in perovskites, by strategically replacing two d-block metallic ions. Basically instead of Pb^{2+}, a B^{1+} mono-valent ion and a B^{III3+} trivalent ion, thus giving a $A_2B^IB^{III}X_6$ type structure .The general structure is shown below in the Fig 1.3.

$AB^{2+}X_3$ — $A_2B^+B^{3+}X_6$

Simple perovskite structure
A = $CH_3NH_3^+$, $CH(NH_2)(NH_2)^+$, Cs^+ etc
B^{2+} = Pb^{2+}
X = Cl^-, Br^-, I^-

Double perovskite structure
A = $CH_3NH_3^+$, $CH(NH_2)(NH_2)^+$, Cs^+ etc
B^+ = Ag^+, Cu^+, Na^+ etc
B^{3+} = Bi^{3+}, Sb^{3+}, In^{3+} etc
X = Cl^-, Br^-, I^-
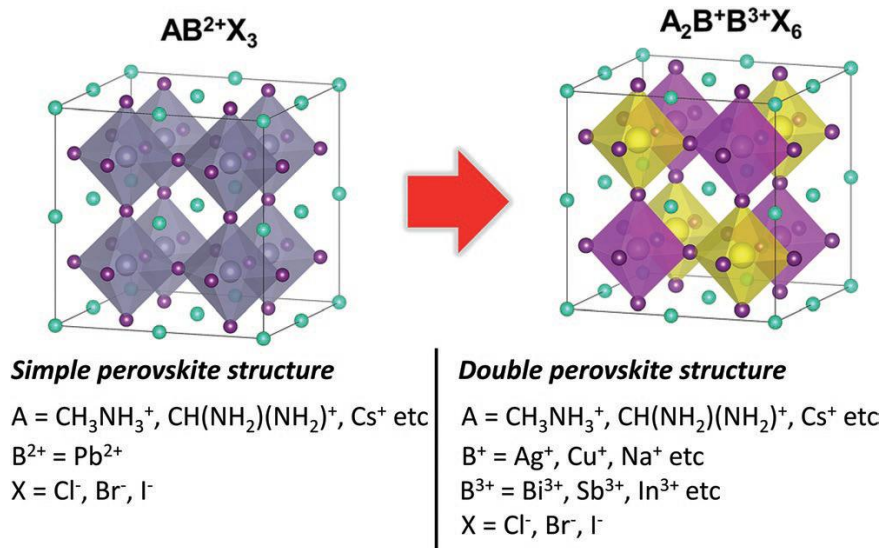
Fig 1.3. Schematic representation of the structures of simple and double perovskites showing the difference in the elemental composition in the B site. [Reproduced from Reference Number 5,6]

The advantage of DP structures is mainly its flexibility for its different composition adjustments. Prospective research in this field is in the directions to improve the optoelectronic properties which help in discovering new Pb-free halide DP. [6]

In this thesis, we study the synthesis of various DP which have a metallic backbone of AgSb, where Ag is the mono-valent ion and Sb is the trivalent ion. By also changing the

A$^+$ mono-valent ion, by not only using Cs$^+$, we observe different properties and changes to the DP.

1.4. Why A$_2$AgSbX$_6$?

Since, Bi and Sb are isoelectronic with lone-pair activity and similar size, thus making it easy to synthesize its analogues using solution based routes. For example the commonly synthesized Cs$_2$AgSbCl$_6$, the Valence Band is mainly accreditted to the Ag 4d, Sb 5s, and Cl 3p states while the Conduction Band primarily is composed of the Ag 5s and Sb 5p states, which can be rationalized o the Br usage as a halide with AgSb in the thesis. On the contrary, the VB to CB transition happens between halide's p states and p states of Sb. Adding to that, the Sb atoms have the Conduction Band-associated charge density mainly locates on it, while the halogens have the VB distribution is localized on it, which enhances the separation of holes and electrons. High photovoltaic performance opportunity is provided by the high electronic dimensionality. [7,8] Fig 1.4 and Fig 1.5. show the structure of Cs$_2$AgSbCl$_6$ and different electronic bands and the different energy levels of it respectively.
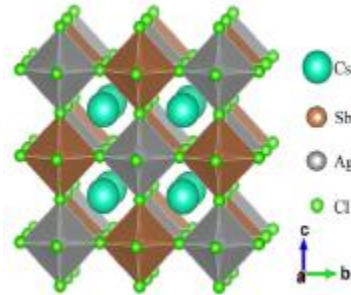
Fig 1.4. Schematic representation of Cs$_2$AgSbCl$_6$ [Reproduced from Reference Number 7]

(a)

Higher Energy States

Conduction Band

Defect State

E' E_0 E_1

Valence Band

(b)

Conduction Band
Sb–5p

Valence Band
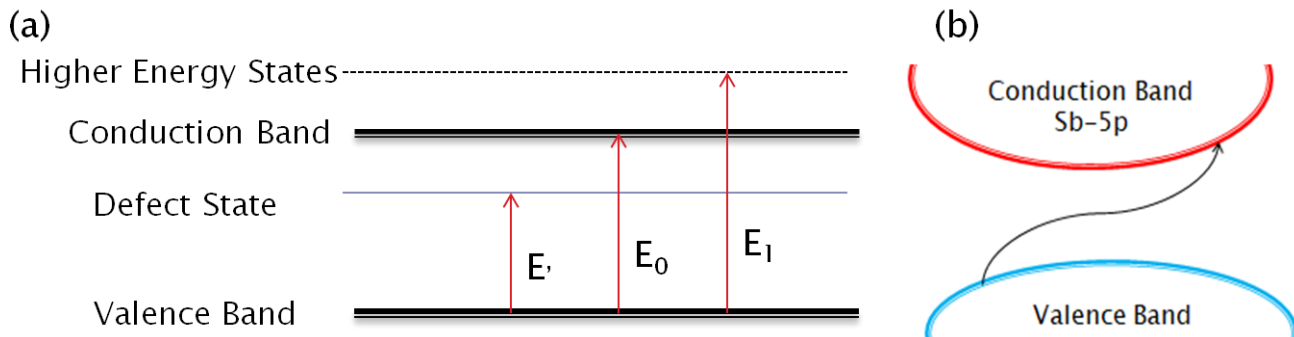
Fig 1.5. (a) Energies of different levels with electronic jumps (b) The movement of holes and electrons from the VBM to Sb-5p energy level. [Reproduced from Reference Number 8]

1.5. Spacer Cations

Organic spacer cations in layered 2D double perovskite with a generalized structure, $(A_1)_2(A_2)_{n-1}B_n X_{3n+1}$ (where A_1 is an organic cation acting as a spacer between the perovskite layers, A_2 is a mono-valent cation) perovskite materials enhance the long-term stability of the resulting PSCs, but affect their power conversion efficiency (PCE) due to poor carrier generation and transportation. Herein, mixed A_1 cations are used in synthesis of layered 2D perovskites to understand the interplay between alkyl amine cations and unsaturated alkyl amine cations [9]. It is proven that alkyl amine spacer cations are capable to initiate and facilitate the precursor assembly, which give rise to the orientated growth of perovskite crystals. Unsaturated alkyl amine cations further lead to reduction of exciton binding energy, which improves carrier pathway in the 2D perovskites [10]. Lets understand with the most common example of PEA^+, PEA^+ is one of the most commonly used spacer cation because of its optimization of solar absorber layer thickness was found to be critical in synthesizing highly efficient 2D perovskite devices with very low hysteresis. The incorporation of larger organic PEA cations into the perovskite framework can largely influence not only the photovoltaic properties but also the stability of the perovskites. There are other multiple reasons of developing 2D Layered Hybrid Inorganic Organic Perovskites (HIOPs) because of their stability and moisture redemption, which are explained in the next section.
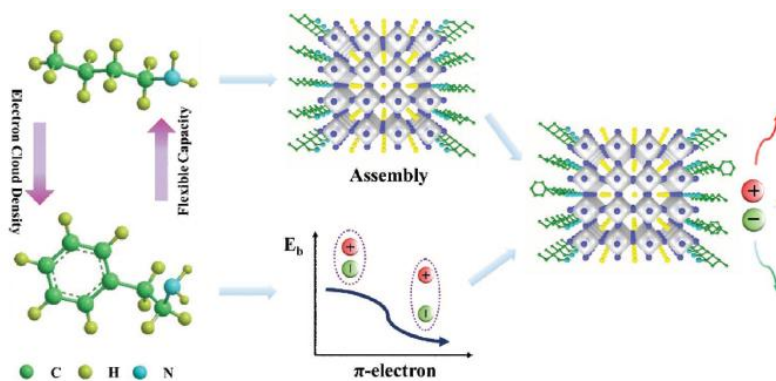
Fig 1.6. Schematic illustration of mechanism via PEA$^+$ introduction into BA based layered perovskite.[Reproduced from Reference Number : 11]

1.6. Hybrid Inorganic Organic Perovskites (HIOPs)

Hybrid organic-inorganic halide perovskite materials have sparked widespread interest due to the richness of their optoelectronic properties. [12] Experimental and hypothetical examinations have proved that their fantastic photovoltaics marginally credited to their astonishing particular electronic properties of $CH_3NH_3PbI_3$, together with the crystal order of the perovskite structure, and the strong Pb 6s-I 5p hostile to holding coupling at the valence band edge. Then, the characteristic thermodynamic unsteadiness of $CH_3NH_3PbI_3$ perhaps begins from the natural cation CH_3NH_3 and its inalienable instability.[13] In a similar vein, the introduction of appropriate large organic spacing cations35 has recently yielded hybrid layered double perovskite halides. [14]

The adaptable properties of few perovskites can be ascribed to the blended points of interest of natural (adaptability, minimal effort) and inorganic (high versatility, crystallinity, and solidness) materials integrated into it. [15]Among the different assortments of crossbreed perovskites, methylammonium lead halide perovskites are the preeminent examined and requested materials. The valence band holes and thus the electronic properties of those materials can be just tuned by powerfully changing the halide, metal, and additionally the natural cations, serving to orchestrate them for suitable for the first applications.[16,17]

These compounds are promising in the sense that (i) a wide range of organic spacing cations can be used; (ii) tunable layer thickness can be achieved, (iii) a metal alloying strategy on both M^{1+} and M^{3+} sites can be carried out; and (iv) varying the halide can be used to control the optoelectronic properties. [18]
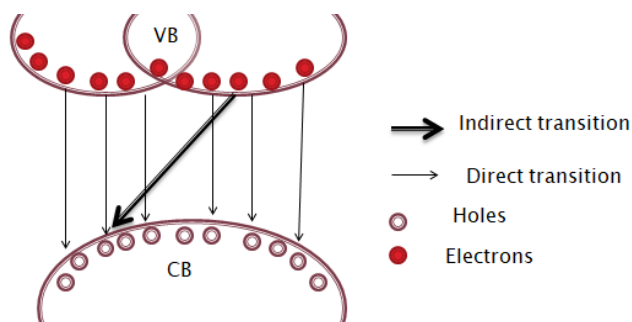
Fig 1.7. Depiction of Direct and Indirect electronic transitions[Reproduced from Reference Number : 19]

1.7. Theory available in the literature

In the vast literature, there are rarely reported HIOPs with A_2AgSbX_6 (A is the spacer cation), but since Sb is isoelectronic to Bi, it can be comparable. There are a few research papers available on $Cs_2AgSbBr_6$, which is synthesized for the comparison to the DPs synthesized using various spacer cations. Concern about double perovskites as photo harvesters would be their relatively large bandgaps, for example, ranging from 1.9eV to 3.3eV. $Cs_2AgBiBr_6$, for example, shows a relatively wide bandgap of 2 eV, which is not suitable for single junction solar cells. Replacing Br by I would lower the conduction band minimum (CBM) and raise the valence band maximum (VBM) due to the interaction between cations and I^- 5p orbitals, forming a much smaller bandgap. However, experimental synthesis of double perovskite iodides has proved to be difficult, with even small amounts of iodine incorporation resulting in the formation of low dimensional phases. An alternative approach is to deploy cations with 5s and 5p (e.g. Sb^{3+}) instead of 6s6p such as Bi^{3+}, to lower the CBM, thus reducing the bandgap. For example, $Cs_2AgSbCl_6$ (2.02 eV) is reported to show a smaller bandgap than $CsAgBiCl_6$ (2.77 eV). [30]

Even though literature suggests that similar band structures for $Cs_2AgSbBr_6$ and $Cs_2AgBiBr_6$, but the Sb 5s and 5p orbitals significantly lower the CBM, thus reducing the bandgap. The absorption edge measured by UV-Vis appears at 1.89 eV, and indicates an indirect transition. The photovoltaic efficiency is low, likely due in part to the presence of secondary phases with larger bandgaps.[30] Fig 1.8 show the molecular energy levels of $Cs_2AgSbBr_6$, where the CBM and VBM are shown. To show that the HOIP is formed, we can confirm by using XRD, where the (110) and (200) peaks are shown at degree 2Θ is at 30°-40° and 40°-50° respectively.
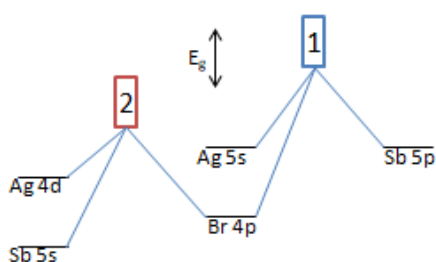
Fig 1.8. Molecular orbital diagram of $Cs_2AgSbBr_6$. The red and blue blocks represent valence band and conduction band, respectively. The numbers 1 and 2 denote the different energy ranges, which show the peaks in PL.[Reproduced from Reference Number : 30]

1.8. Problems that are addressed in the thesis

With the aim of synthesizing and understanding of hybrid layered double perovskite halides, and to gain insight into crystal structure, we demonstrate that a large family of cation-ordered hybrid double-perovskite halides can be obtained through the judicious selection of a range of organic spacer cations. The selection of spacer cations were done in such a way that there is at least one $-NH_2$ group at the terminal end of its hydrocarbon chain. An attempt to materialize different types of spacer cations (whether they can act as spacer cations) to synthesize different types of HIOPs using an AgSb backbone.

The choice of usage as Br^-, is due to the fact that, the optical properties are highly tunable, through varying the layer thickness, increasing the length of the organic and alloying the metal (M^{III}). Here, we study and synthesize different DPs with multiple spacer ions and M^{III} is Sb^{3+}.

CHAPTER 2 - CHARACTERISATION TECHNIQUES

2.1. PHOTOLUMINESCENCE SPECTROSCOPY

Photoluminescence (abbreviated as PL) is light emission from any variety of matter once the absorption of photons (electromagnetic radiation). It's initiated by photons that excite electrons to a higher energy level in an atom. In the same light, light is shown onto a sample, where it's absorbed and where the photo-excitation process happens. The photo-excitation causes the sample to leap to a higher electronic state, and can unleash its energy, (photons) because it relaxes and returns to back to a lower energy level. The emission of light or luminescence through this method is called photoluminescence, PL. During this work, time-resolved photoluminescence technique is applied. [20]

The working of a Photoluminescence spectrometer is as follows, the sample is irradiated at one wavelength and emission is observed over a range of wavelengths. The excitation monochromator selects the excitation wavelength and the emission monochromator selects one wavelength at a time to observe. The basic schematic representation of a photometer is depicted in the Fig 2.1. [21]
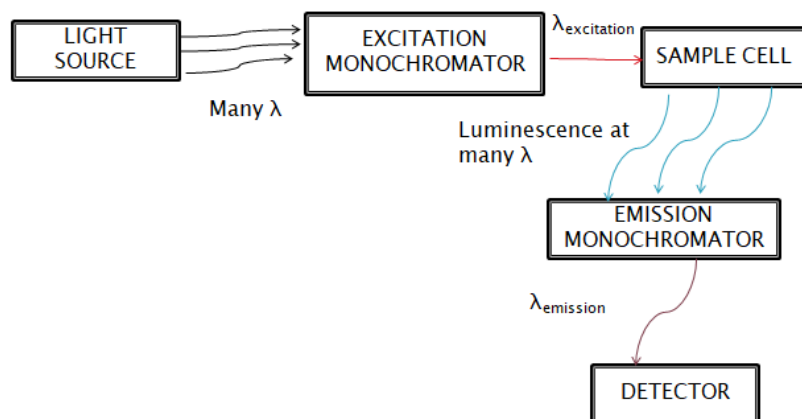

Fig 2.1. Basic schematic representation of Spectrophotometer in PL. [Reproduced from Reference Number: 22]

2.2. UV-VIS SPECTROSCOPY

UV-Vis spectroscopy (UV–Vis or UV/Vis) alludes to ingestion spectroscopy or reflection spectroscopy halfway of the bright and along these lines full, adjoining obvious ghastly areas. Compounds containing bonding and non-bonding electrons (n-electrons) will ingest vitality in the sort of bright or noticeable light to energize these electrons to a higher enemy of holding sub-atomic orbitals. The part just energized the electrons (for example lower vitality hole between the HOMO and in this manner LUMO), the more drawn out the frequency of light it will assimilate. There are four feasible kinds of changes (π–π^*, n–π^*, σ–σ^*, and n–σ^*), and that they can be requested as follows: σ–σ^* > n–σ^* > π–π^* > n–π^*. [23]
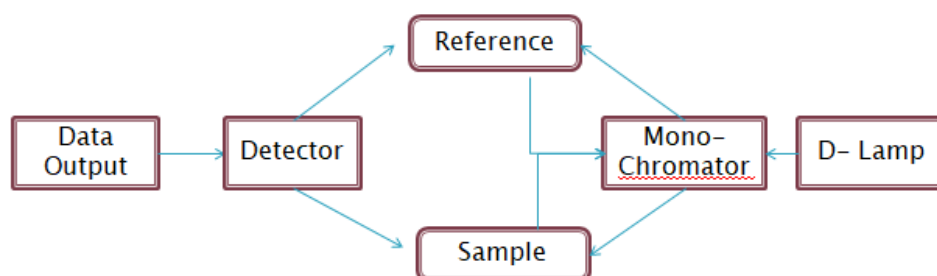
Fig 2.2. Simplified schematic of a double beam UV–visible spectrophotometer[Reproduced from Reference Number : 24]

The Beer-Lambert law states that the absorbance of a solution is directly proportional to the concentration of the absorbing species in the solution and the path length. Thus, for a fixed path length, UV/Vis spectroscopy can be used to determine the concentration of the absorber in a solution. It is necessary to know how quickly the absorbance changes with concentration. This can be taken from references, or more accurately, determined from a calibration curve. [25]

The method is most often used in a quantitative way to determine concentrations of an absorbing species in solution, using the Beer–Lambert law:

$$A = \varepsilon.c.l = \log_{10}(I_0/I) \qquad\qquad (2.3)$$

where A is the measured absorbance (in Absorbance Units (AU)), I_o is the intensity of the incident light at a given wavelength, I is the transmitted intensity, l the path length through the sample, and c the concentration of the absorbing species. For each chemical compound or element and a particular wavelength, ε is a constant which is known as the molar absorptivity or extinction coefficient. [25]

2.3. X-RAY DIFFRACTION

X-ray diffraction is a technique used for the determination structure of crystalline materials. When a crystalline material is exposed to beam of incident X-rays, the incident X-rays are diffracted to several specific directions. By measurement of the angles and intensities of those diffracted beams, crystal structure of the material can be determined.

X-rays are diffracted by a crystalline material following Bragg's law as stated below:

$$n\lambda = 2d_{hkl}\sin\theta \qquad\qquad (2.4)$$

Where n is an integer called the order of reflection, λ is the wavelength of the radiation, d_{hkl} is the inter-planar spacing (the perpendicular separation) of the (hkl) planes and θ is the diffraction angle or Bragg angle (Equation. 2.4). [26]
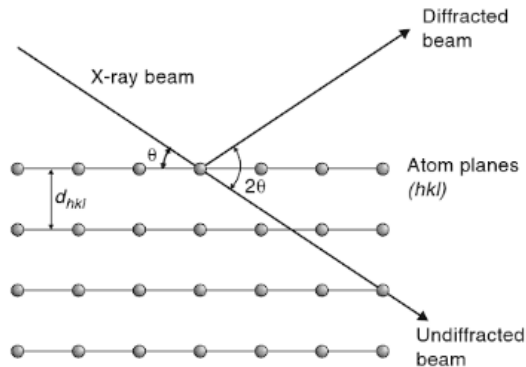

Fig. 2.3. The geometry of Bragg's law for the diffraction of X-rays from a set of crystal planes, (hkl), with interplanar spacing d_{hkl} [Reproduced from Reference Number: 27]

The Bragg condition, applied to diffraction information, gives us in a rundown of $dhkl$ values for a compound. It is feasible, by embeddings these to informational indexes

joined, to scale the size of the unit cell of the material giving the diffraction design. There are for the most part two sorts of diffraction methods: powder X-Ray diffraction and crystal X-Ray diffraction, between where the powder one is the most generally utilized. Powder X-Ray diffraction works under the conviction that the example is arbitrarily orchestrated. Accordingly, a factually indispensable number of each plane of the crystal structure will be in the best possible direction to diffract the X-Ray. [27]
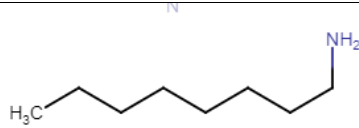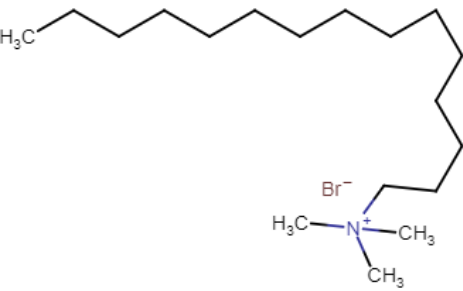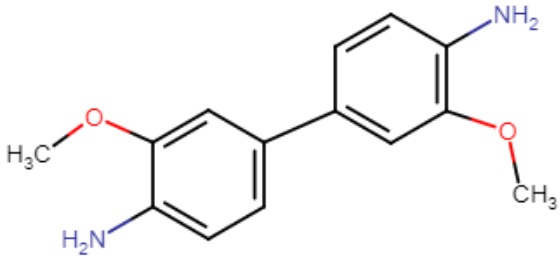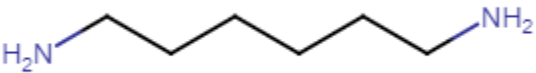
The XRD example can be taken and recorded with a diffractometer comprising of 3 primary components: an X-ray tube, an sample holder, and an X-ray detector (Fig. 2.5). X-ray beams are produced in a cathode ray tube by passing current through a Tungsten filament, which emits electrons in the evacuated chamber. A very high potential difference (few kV) is applied to accelerate the electrons towards anode. [34] The fast moving electrons collide with the anode and knocks off one electron from the K shell of the anode material. Then the electron from the L shell jumps down to the K shell thereby emitting a characteristic X-ray energy. For powder X-ray diffraction , copper is used as the anode in the X-ray tube. CuKα radiation has a wavelength of 1.5418Å.[28]

When the X-rays are illuminated onto the sample, with the circulation of the sample and detector, the intensity of the reflected X-rays is noted. Once the angle of the incident X-rays bombarding the sample comes in place with the Bragg Equation, constructive interference happens and a peak in intensity occurs. A detector records and processes this X-ray signal and converts the signal to a count rate. The angle of an X-ray diffractometer is such the sample rotates in the path of the accurately parallel to the X-ray beam at an angle θ whereas the X-ray detector is attached on an arm to collect the diffracted X-rays and rotates at an angle of 2θ. For typical powder patterns, data is collected at 2θ from ~5° to 70°. [29]

CHAPTER 3 – SYNTHESIS, CHARACTERISATION AND SUMMARY

3.1. STARTING MATERIALS

The thesis is based on usage of spacer cations to synthesize OIHPs, the following spacer cations were used.

Sl.No.	Spacer Name	Spacer Structure
1.	1- Octyl-Amine	
2.	CTAB	
3.	3,3'-Dimethoxybiphenyl-4,4'-diamine (Dimethoxy Benzidine/ o-Anisidine)	
4.	1,6-Diamine Hexane	
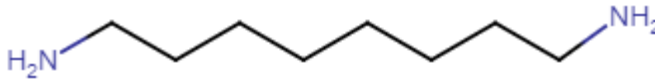
5.	1,8-Diamine Octane	

Table 3.1. Spacer cations used.

The following table shows the ratio of the starting materials used to create the 2D Layered Perovskites according to the serial number of spacer mentioned above.

Sl.No.	Name	CsBr	AgBr	SbBr$_3$	Spacer	HBr	Solvents
1	Cs$_2$AgSbBr$_6$	75 μg	64 μg	123 μg	n/a	600 μl	n/a
2	Mn doped Cs$_2$AgSbBr$_6$	75 μg	64 μg	123 μg	n/a	600 μl	MnBr2 - 120 μg
3	(OA)$_2$AgSbBr$_6$	n/a	40 μg	76 μg	350 μl	500 μl	H$_2$0 - 100 μl
4	(OA)CsAgSbBr$_6$	27 μg	24 μg	46 μg	700 μl	700 μl	MeOH - 350 μl
5	(CTAB)$_2$AgSbBr$_6$	n/a	72 μg	137 μg	384.3 μg	100 μl	H$_2$0 - 250 μl
6	(o-Anisidine)AgSbBr$_6$	n/a	72mg	137mg	1905μg	500 μl	H$_2$0 - 2000 μl
7	(1,6-Diamino hexane)AgSbBr$_6$	n/a	72mg	137mg	9mg	500 μl	H$_2$0 - 2000 μl
8	(1,8-Diamino octane)AgSbBr$_6$	n/a	72mg	137mg	10mg	500 μl	H$_2$0 - 2000 μl

Table 3.2. Amount of starting materials required.

3.2. SYNTHESIS

The most preferred and used method is the solution method or the hot-injection method. Here, to have a clean environment the Schlenk Line was used. A 3-neck Round Bottom flask was used initially inserting the Bromides were added carefully as $SbBr_3$ is toxic, and mixed well using a magnetic stirrer and a magnetic bead till an even mixture was formed. Then, vacuum was created using the apparatus, following that the spacer, HBr and H_2O were added and rotated well. Slowly at a rate of 5° C/min was incremented till 100° C- 120° C. The vacuum was turned off and immediately N_2 gas flushed inside slowly and the temperature was incremented to $150\,^o$ C – $160\,^o$ C at the same rate. There were 2 ways of cooling both done under the influence of N_2 gas, firstly the fast cooling by dipping in a cold water bath tub and secondly by decreasing the magnetic stirrer at $5\,^o$ C / hour which generally helped to get crystals.
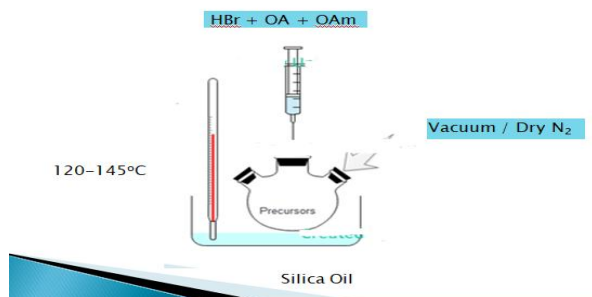
Fig 3.1. Hot injection method Synthesis
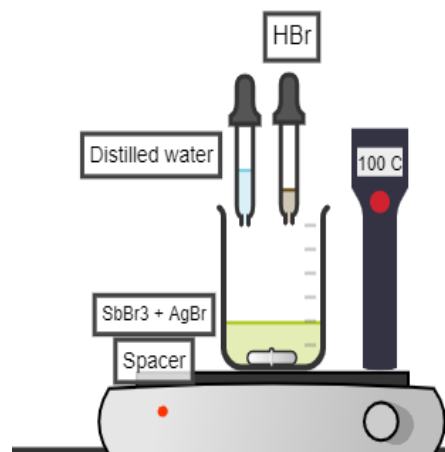
Fig 3.2. Solution State

3.3. CHARACTERISATION

3.3.1. Cs$_2$AgSbBr$_6$

Fig 3.3.1. (a) PL Spectra, (b) UV-Vis Spectra, (c) XRD (d) Tauc Plot of Cs$_2$AgSbBr$_6$

The excitation wavelength for PL spectra was kept at 360 nm. In the PL spectra plot, the lower absorption peak and higher energy absorption peak are for the most part credited to the optical change from Br 4p to Sb 5p and Ag 4d to Sb 5p, individually[as shown in Fig 1.8].[30]

The (100), (110) and (200) peak with high intensity agrees well with the theory, showing the formation of the corresponding crystalline planes and the perovskite rock-salt structure. [37] From the above given Tauc plot we can see that the bandgap of the perovskite formed is 1.87eV, when compared to Cs$_2$AgSbCl$_6$ which has 2.60 eV, but is very close to Cs$_2$AgSbBr$_6$ which is theoretically 1.90eV [30].

The UV-Vis Spectrum shows a band edge emission of 360 eV, which is the allowed transition from the third Valence Band (VB) to the Conduction Band (CB). The broad pre-300 nm peak shows the forbidden transitions between the 1st and 2nd VB to that of the CB [as shown in Fig 1.5].

3.3.2. Mn doped Cs₂AgSbBr₆

Fig 3.3.2. (a) PL Spectra, (b) UV-Vis Spectra, (c) XRD, (d) Tauc plot of Mn doped Cs₂AgSbBr₆

The excitation wavelength for PL spectra was kept at 360 nm. In the PL spectra plot, the lower absorption peak at 442nm and higher energy absorption peak at 573nm are for the most part credited to the optical change from Br 4p to Sb 5p and Ag 4d to Sb 5p, individually[as shown in Fig 1.8]. The sharp peak at 570nm shows the presence of Mn in the compound confirming its doping. [30]

The (100), (111) and (200) peak with high intensity agrees well with the theory, showing the formation of the corresponding crystalline planes and the perovskite rock-salt structure. [37] From the above given Tauc plot we can see that the bandgap of the perovskite formed is 2.82 eV, which is can be made favorable for further experimental uses to produce OIHPSC because its bandgap is slightly less when compared to Cs₂AgSbCl₆ which has 2.60 eV and is very close to Cs₂AgSbBr₆ which is theoretically 1.90eV [30].

.

The UV-Vis Spectrum shows a band edge emission of 365 eV, which is the allowed transition from the third Valence Band (VB) to the Conduction Band (CB). The broad pre-300 nm peak shows the forbidden transitions between the 1st and 2nd VB to that of the CB [as shown in Fig 1.5].
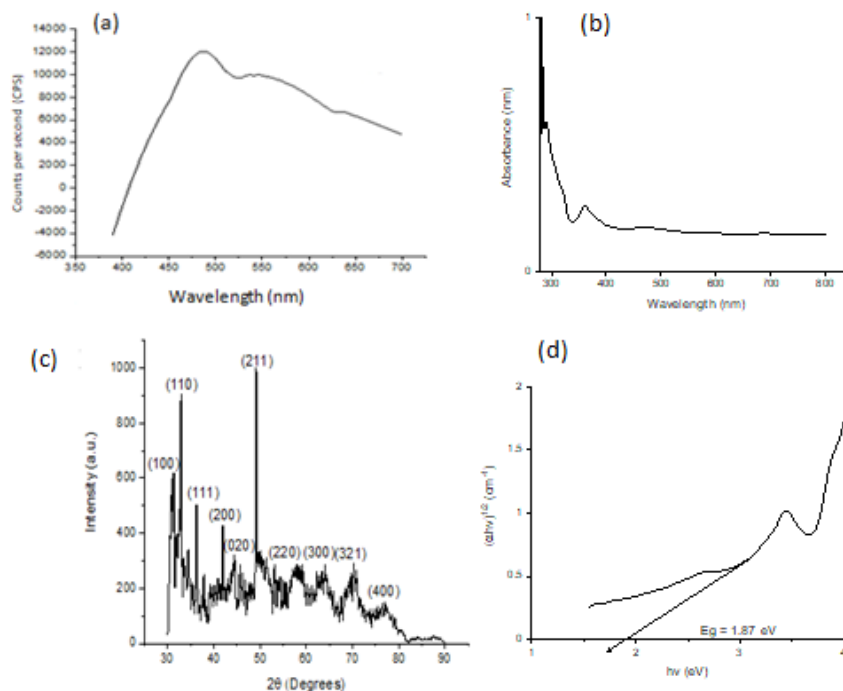
3.3.3. $(OA)_2AgSbBr_6$

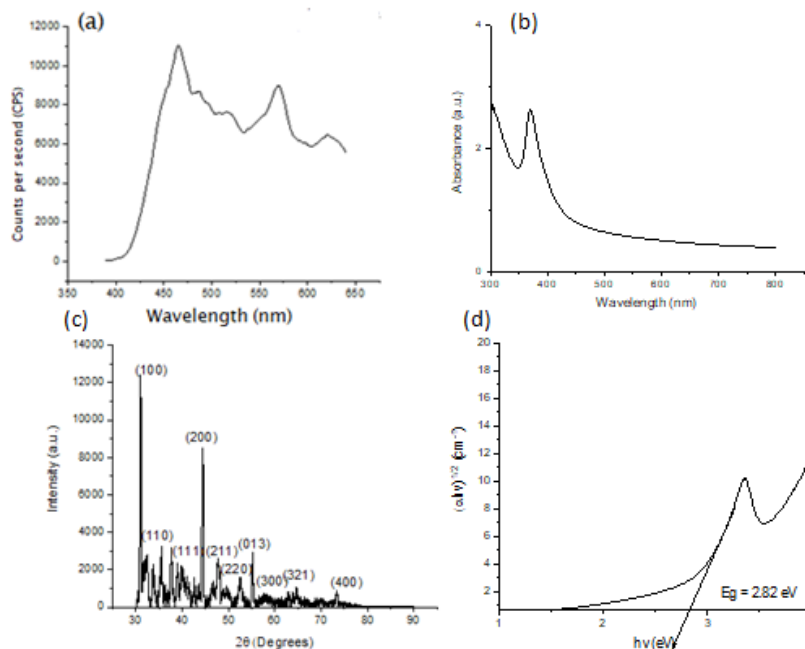**Fig 3.3.3. (a) PL Spectra, (b)UV-Vis Spectra, (c) XRD, (d) Tauc Plot of $(OA)_2AgSbBr_6$**

The excitation wavelength for PL spectra was kept at 360 nm. In the PL spectra plot, the lower absorption peak at 435nm and higher energy absorption peak at 560nm are for the most part credited to the optical change from Br 4p to Sb 5p and Ag 4d to Sb 5p, individually[as shown in Fig 1.8]. [30]

The (100), (110) and (200) peak with high intensity agrees well with the theory, showing the formation of the corresponding crystalline planes, presence of hydrocarbon spacer cation and the perovskite rock-salt structure. [37] From the above given Tauc plot we can see that the bandgap of the perovskite formed is 2.72 eV, which is favorable for further

experimental uses to produce OIHPSC because its bandgap is similar when compared to $Cs_2AgSbCl_6$ which has 2.60 eV.

The UV-Vis Spectrum shows a band edge emission of 365 eV, which is the allowed transition from the third Valence Band (VB) to the Conduction Band (CB). The broad pre-300 nm peak shows the forbidden transitions between the 1st and 2nd VB to that of the CB [as shown in Fig 1.5].

3.3.4. (OA)CsAgSbBr$_6$

Fig 3.3.4. (a) PL Spectra, (b) UV-Vis Spectrum, (c) Tauc Plot of (OA)CsAgSbBr$_6$

The excitation wavelength for PL spectra was kept at 360 nm. In the PL spectra plot, the lower absorption peak isn't observed may be due to less concentration and low counts, whereas the higher energy absorption peak at 570nm are for the most part credited to the optical change from Br 4p to Sb 5p and Ag 4d to Sb 5p, individually[as shown in Fig 1.8]. [30]

The (100), (110), and (200) peak with high intensity agrees well with the theory, showing the formation of the corresponding crystalline planes, presence of space cation and the

perovskite rock-salt structure. [37] From the above given Tauc plot we can see that the bandgap of the perovskite formed is 2.62 eV.

The UV-Vis Spectrum shows a band edge emission of 360 eV, which is the allowed transition from the third Valence Band (VB) to the Conduction Band (CB). The broad pre-300 nm peak shows the forbidden transitions between the 1st and 2nd VB to that of the CB [as shown in Fig 1.5].
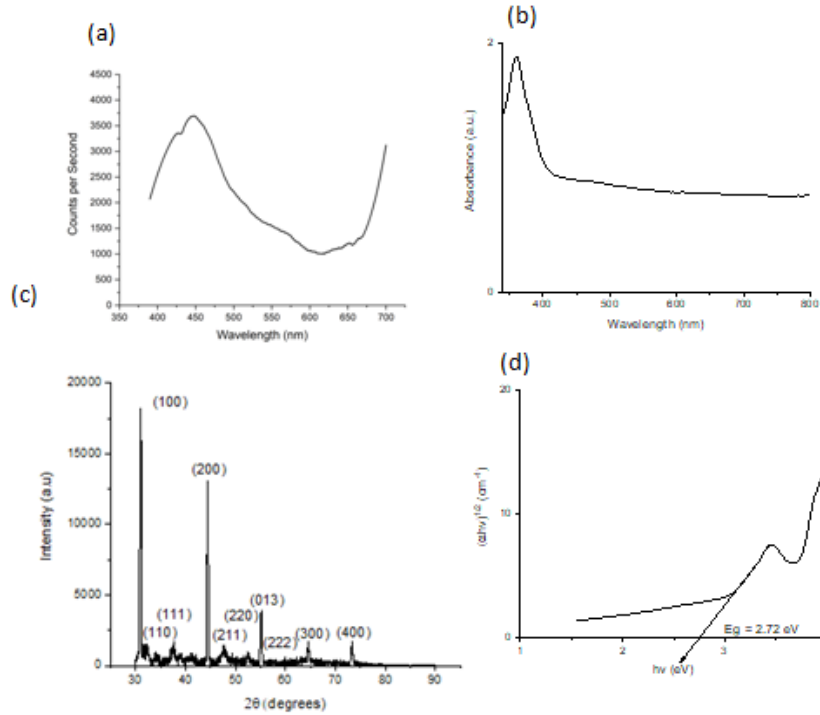
3.3.5. $(CTAB)_2AgSbBr_6$

Fig 3.3.5. (a) PL Spectra, (b) UV-Vis Spectrum, (c) Tauc Plot of $(CTAB)_2AgSbBr_6$

The excitation wavelength for PL spectra was kept at 360 nm. In the PL spectra plot, the lower absorption peak isn't observed may be due to less concentration and low counts, whereas the higher energy absorption peak at 565nm are for the most part credited to the optical change from Br 4p to Sb 5p and Ag 4d to Sb 5p, individually[as shown in Fig 1.8]. [30]

The (100), (110) and (200) peak with high intensity agrees well with the theory, showing the formation of the corresponding crystalline planes, presence of hydrocarbon spacer cation and the perovskite rock-salt structure. [37] From the above given Tauc plot we can see that the bandgap of the perovskite formed is 2.80 eV, which is not favorable for further experimental uses to produce OIHPSC because its bandgap is pretty low when compared to $Cs_2AgSbCl_6$ which has 2.60 eV.

The UV-Vis Spectrum shows a band edge emission of 355 nm, which is the allowed transition from the third Valence Band (VB) to the Conduction Band (CB). The broad pre-300 nm peak shows the forbidden transitions between the 1st and 2nd VB to that of the CB [as shown in Fig 1.5].
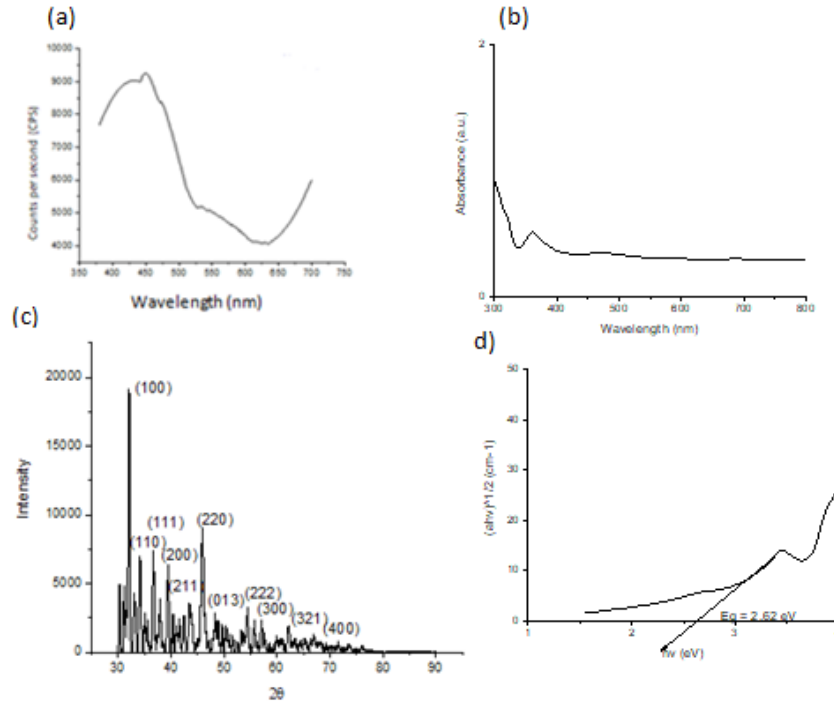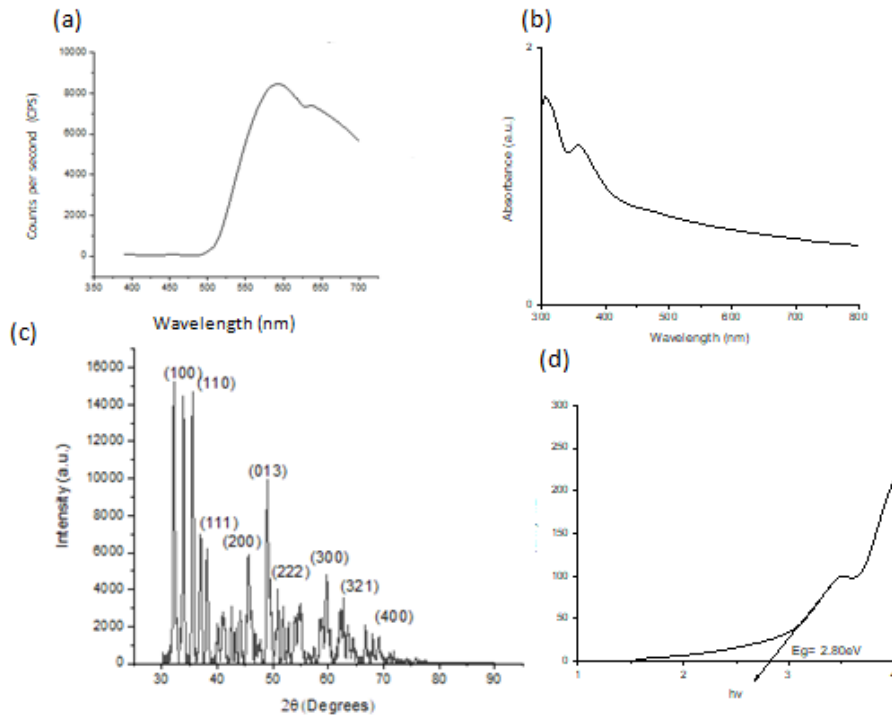
3.3.6. O-Dianisidine

Fig 3.3.6. (a) PL Spectra, (b)UV-Vis Spectra, (c) XRD, (d) Tauc Plot of (o-Anisidine)AgSbBr$_6$

The excitation wavelength for PL spectra was kept at 360 nm. In the PL spectra plot, the lower absorption peak at 455nm and higher energy absorption peak at 535nm are for the most part credited to the optical change from Br 4p to Sb 5p and Ag 4d to Sb 5p, individually[as shown in Fig 1.8]. [30]

The (100), (110) and (200) peak with high intensity agrees well with the theory, showing the formation of the corresponding crystalline planes, spacer cation presence and the perovskite rock-salt structure. [37] From the above given Tauc plot we can see that the bandgap of the perovskite formed is 3.17 eV. Which is not favorable for further experimental uses to produce OIHPSC because its bandgap is pretty high when compared to $Cs_2AgSbCl_6$ which has 2.60 eV.

The UV-Vis Spectrum shows a band edge broad pre-300 nm peak shows the forbidden transitions from the 1st and 2nd VB to that of the CB [as shown in Fig 1.5].

3.3.7. 1,6 Diamine Hexane

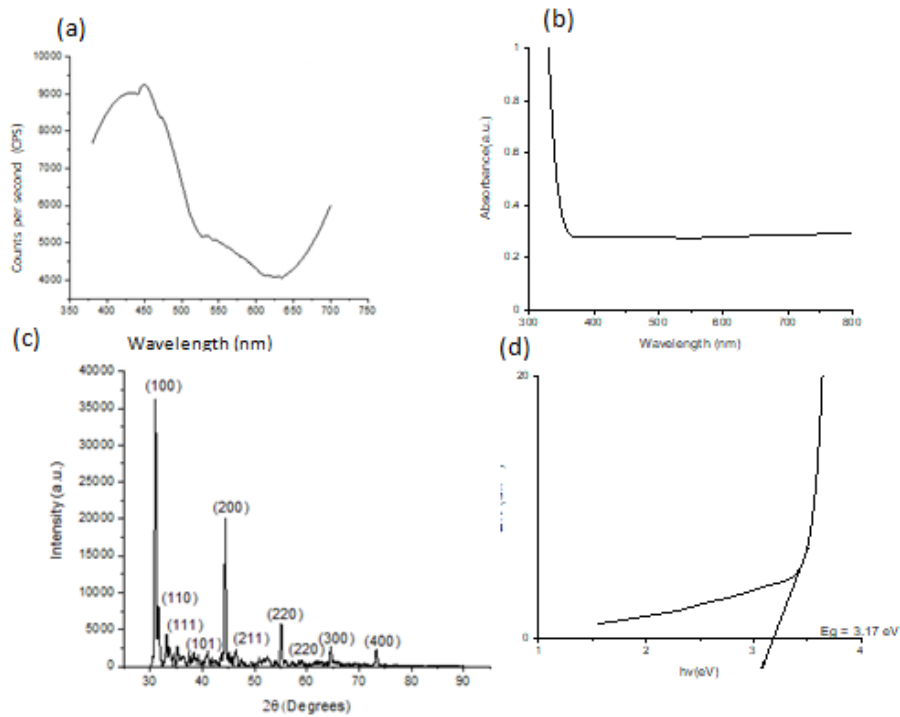Fig 3.3.7. (a) PL Spectra, (b)UV-Vis Spectra, (c) XRD, (d) Tauc Plot of (1,6-Diamino hexane)AgSbBr$_6$

The excitation wavelength for PL spectra was kept at 360 nm. In the PL spectra plot, the lower absorption peak at 475nm and higher energy absorption peak at 535nm are for the most part credited to the optical change from Br 4p to Sb 5p and Ag 4d to Sb 5p, individually[as shown in Fig 1.8]. [30]

The (100), (110) and (200) peak with high intensity agrees well with the theory, showing the formation of the corresponding crystalline planes, presence of organic moiety spacer and the perovskite rock-salt structure. [37] From the above given Tauc plot we can see that the bandgap of the perovskite formed is 2.72 eV, which is favorable for further experimental uses to produce OIHPSC because its bandgap is closer to $Cs_2AgSbCl_6$ which has 2.60 eV.

The UV-Vis Spectrum shows a band edge broad pre-300 nm peak shows the forbidden transitions from the 1st and 2nd VB to that of the CB [as shown in Fig 1.5].

3.3.8. 1,8- Diamine Octane

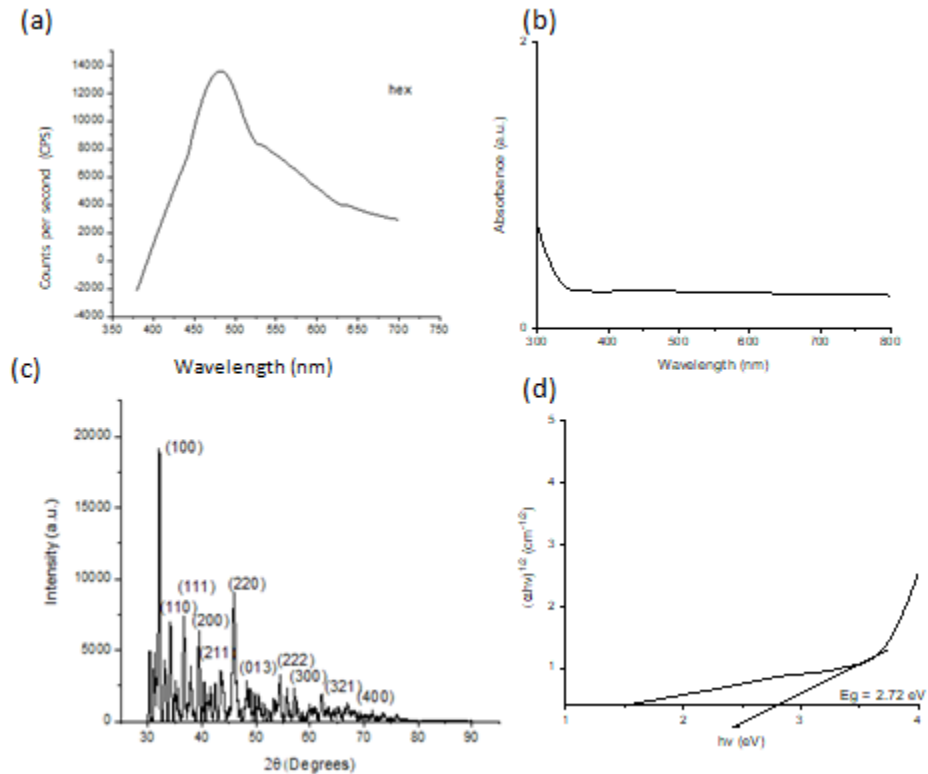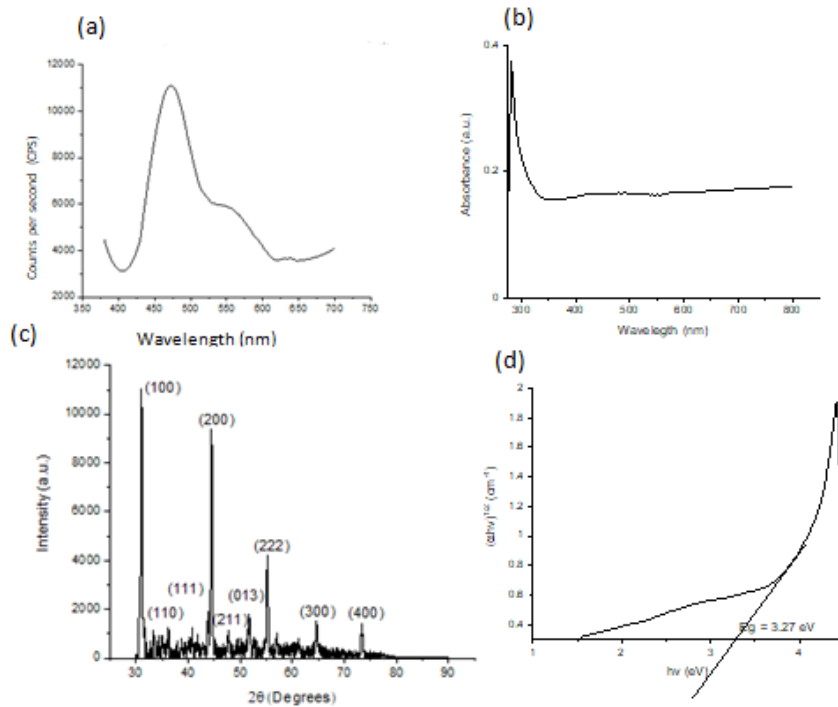**Fig 3.3.8(a) PL Spectra, (b)UV-Vis Spectra, (c) XRD, (d) Tauc Plot of (1,8-Diamino octane)AgSbBr$_6$**

The excitation wavelength for PL spectra was kept at 360 nm. In the PL spectra plot, the lower absorption peak at 475nm and higher energy absorption peak at 555nm are for the most part credited to the optical change from Br 4p to Sb 5p and Ag 4d to Sb 5p, individually[as shown in Fig 1.8]. [30]

The (100), (110) and (200) peak with high intensity agrees well with the theory, showing the formation of the corresponding crystalline planes, presence of organic moiety spacer cation and the perovskite rock-salt structure. [37] From the above given Tauc plot we can see that the bandgap of the perovskite formed is 3.27 eV, which is favorable for further experimental uses to produce OIHPSC because its bandgap is closer to $Cs_2AgSbCl_6$ which has 2.60 eV.

The UV-Vis Spectrum shows a band edge emission of 360 eV, which is the allowed transition from the third Valence Band (VB) to the Conduction Band (CB). The broad pre-300 nm peak shows the forbidden transitions between the 1st and 2nd VB to that of the CB[as shown in Fig 1.5].

3.4. SUMMARY AND OUTLOOK

Lead halide perovskites have been the key source and preliminary step in developing PV technologies. It has been a huge deal in synthesizing, processing and developing these materials which have good power conversion efficiency for a solar cell. The basic structure of the perovskite is an ortho-rhombic structure of $APbX_3$, where A is monovalent cation of s-block elements such as Cs^+, and X is a halide. But, due to the toxicity of Pb to the nature, there is a wide quest of developing perovskites in an alternative form. One of the main solutions to this problem is creating a DP (Double Perovskite) where the +2 ion of Pb is replaced by 2 cations, a monovalent ion like Ag^+ and a trivalent cation like Sb^{3+}. These when combined give a similar characteristic of the $APbX_3$ structure, which have a common formula of $A_2M^1M^2X_6$, where M^1 is like Ag^+, and M^2 is like Sb^{3+}. The reason of choosing Sb is due to its isoelectronic properties to Bi, as there much AgBi backbone of DPs which have been synthesized and reported, which have similar or better properties when to compared to Lead-based Perovskites.

Perovskites which are OIHPs have emerged as a low-cost and high-efficiency thin-film photovoltaic (PV) technology, due to the production cost inorganic DPs. OIHPs are non-toxic and very easily synthesized. Spacer cations are used for the organic part of the OIHPs. Generally, a spacer cation is a long hydrocarbon saturated or unsaturated chain

with an amine group that provides the positive ion if A^+ in the $A_2M^1M^2X_6$ DP structure. The amino group can act as the $-NH_3^+$ ion in the solvents.

In this thesis, different spacer cations were used such as 1-Octylamine, CTAB, o-Anisidine, 1,6-DiaminoHexane and 1,8-DiaminoOctane and compared its properties with $Cs_2AgSbBr_6$ and also Mn doped $Cs_2AgSbBr_6$. As from the characterization we can observe usage of spacer cations helped in improve the bandgap of the perovskites and also Mn doping too when compared to $Cs_2AgSbBr_6$. So, we can conclude positively that usage of spacer ions and doping with Mn can help improve bandgap of perovskites. We determine that the broad, lowest-energy direct transition in some perovskites occur between nominally inorganic-derived states at band extrema and propose that the lack of considerable band-edge PL likely derives from spatial localization/separation of photo excited holes and electrons in the vicinity of Ag and Sb, respectively. But on the contrary, we should also test for the degradation of these perovskites, as there is usage of organic materials which tend to degenerate at high temperatures and also importantly upon fabrication, whether these provide effective PCE when compared to its inorganic and lead counterparts.

In conclusion, one can say that it's important for one to find alternative and effective sources of renewable energy, when there is in need due to the consequential deterioration of fossil fuels and natural energy.

BIBLIOGRAPHY

[1] UN Statistics, Regional UK Statistics 2003-2016 :
https://www.gov.uk/government/statistics/ regional-renewable-statistics,
2017.

[2] A History of Perovskite Solar Cells : http://blog.bccresearch.com/a-history-of-perovskite-solar-cells

[3] Double Perovskites : https://www.cpfs.mpg.de/2486283/Double-perovskites

[4] A.R. West, Solid State Chemistry and Its Applications, 2nd Edition, 1991, Wiley, UK.

[5] Q. Huang, J. W. Lynn, R. W. Erwin, J. Jarupatrakorn and R. J. Cava, Oxygen Displacements and Search for Magnetic Order in Sr^{3+} *Physical Review B*, 58 (1998) 8515-8521.

[6] G.D. Niu, X.D. Guo, L.D. Wang. Review of Recent Progress in Chemical Stability of Perovskite Solar Cells. Journal of Materials Chemistry A. 2015, 8970-8980.

[7] N.-G. Park. Perovskite solar cells: An emerging photovoltaic technology. Materials Today, 18(2):65–72, 2015.

[8] Protesescu, L.; Yakunin, S.; Bodnarchuk, M. I.; Krieg, F.; Caputo, R.; Hendon, C. H.; Yang, R. X.; Walsh, A.; Kovalenko, M. V. Nanocrystals of Cesium Lead Halide Perovskites (CsPbX3, X = Cl, Br, and I): Novel Optoelectronic Materials Showing Bright Emission with Wide Color Gamut. Nano Lett. 2015, 15, 3692−3696.

[9] Deepak Thrithamarassery Gangadharan, Yujie Han, Ashish Dubey, Aromatic Alkylammonium Spacer Cations for Efficient Two-Dimensional Perovskite Solar Cells with Enhanced Moisture and Thermal Stability Sol. RRL 2018, Vol. 2 Issue 4, 1700215

[10] L. C. Schmidt, A. Pertegas, S. Gonzalez-Carrero, O. Malinkiewicz, S. Agouram, G. M. Espallargas, H. J. Bolink, R. E. Galian, J. Perez-Prieto, Nontemplate synthesis of CH3NH3PbBr3 perovskite nanoparticles. *J. Am. Chem. Soc.* 2014, *136*, 850-3.

[11] F. Hao, C. C. Stoumpos, R. P. H. Chang, M. G. Kanatzidis, Anamalous Bandgap Behavious of Sn and Pb Perovskites, *J. Am. Chem. Soc.* 2014, *136*, 8094-8099;

[12] Era, M., Morimoto, S., Tsutsui, T. & Saito, S. Organic–inorganic heterostructure electroluminescent device using a layered perovskite semiconductor (C6H5C2H4NH3)2PbI4. Appl. Phys. Lett. 65, 676–678 (1994).

[13] H. Y. Jeong, J. Y. Kim, J. W. Kim, J. O. Hwang, J.-E. Kim, J. Y. Lee, T. H. Yoon, B. J. Cho, S. O. Kim, R. S. Ruoff, S.-Y. Choi, Thin film oxides of perovskites, *Nano Lett.* 2010, *10*, 4381-4396;

[14] Haining Chen and Shihe Yang. Stabilizing and scaling up carbon-based perovskite solar cells. Journal of Materials Research, 32(16):3011–3020, 2017.

[15] P. P. Boix, K. Nonomura, N. Mathews, S. G. Mhaisalkar, Current Progress and Future perpective of OIHPs, *Mater.Today* 2014, *17*, 16;

[16] Kikuchi, K., Takeoka, Y., Rikukawa, M. & Sanui, K. Fabrication and characterization of organic–inorganic perovskite films containing fullerene derivatives. Colloids Surf. A 257-258, 199–202 (2005).

[17] K. Wojciechowski, M. Saliba, T. Leijtens, A. Abate, H.J. Snaith. Sub-150 C processed meso-superstructured perovskite solar cells with enhanced efficiency. Energy & Environmental Science. 2014, 7 (3), 1142-1147.

[18] Soe, C. M. M.; Nie, W.; Stoumpos, C. C.; Tsai, H.; Blancon, J.-C.; Liu, F.; Even, J.; Marks, T. J.; Mohite, A. D.; Kanatzidis, M. G. Understanding Film Formation Morphology and Orientation in High Member 2D Ruddlesden−Popper Perovskites for High-Efficiency Solar Cells. Adv. Energy Mater. 2018, 8, 1700979.

[19] Kulbak, M.; Cahen, D.; Hodes, G. How Important Is the Organic Part of Lead Halide Perovskite Photovoltaic Cells? Efficient CsPbBr3 Cells. J. Phys. Chem. Lett. 2015, 6, 2452−2456.

[20] Z.H. W, H.N. Chen, K.Y. Yan, S.H. Yang. Inkjet Printing and Instant Chemical Transformation of a $CH_3NH_3PbI_3$/Nanocarbon Electrode and Interface for Planar Perovskite Solar Cells. Chemie International Edition, 2014, 53, 13239

[21] Xu, Z. et al. Phase transition control for high performance Ruddlesden–Popper perovskite solar cells. Adv. Mater. 30, 1707166 (2018).

[22] Quan, L. N.; Zhao, Y.; García de Arquer, F. P.; Sabatini, R.; Walters, G.; Voznyy, O.; Comin, R.; Li, Y.; Fan, J. Z.; Tan, H.; Pan, J.; Yuan, M.; Bakr, O. M.; Lu, Z.; Kim, D. H.; Sargent, E. H. Tailoring the Energy Landscape in Quasi-2D Halide Perovskites Enables Efficient Green-Light Emission. Nano Lett. 2017, 17, 3701−3709.

[23] Byun, J.; Cho, H.; Wolf, C.; Jang, M.; Sadhanala, A.; Friend, R. H.; Yang, H.; Lee, T. W. Efficient Visible Quasi-2D Perovskite Light- Emitting Diodes. Adv. Mater. 2016, 28, 7515−7520.

[24] Time Resolved PL : https://www.picoquant.com/applications/category/materials-science/time-resolved-photoluminescence#description

[25] Working of TRPL : http://www.cappa.ie/advanced-research/techniques/time-resolved-photoluminescence/

[26] W.K. Metzger, R.K. Ahrenkiel, P. Dippo, J. Geisz, M.W. Wanlass, S. Kurtz. Time-Resolved Photoluminescence and Photovoltaics. 2004 DOE Solar Energy Technologies Program Review Meeting

[27] Skoog, Douglas A.; Holler, F. James; Crouch, Stanley R. (2007). *Principles of Instrumental Analysis* (6th ed.). Belmont, CA: Thomson Brooks/Cole. pp. 169–173.

[28]UV-Vis Spectroscopy: https://www.jove.com/science-education/10204/ultraviolet-visible-uv-vis-spectroscopy

[29]Visible and Ultra-violet Spectroscopy: https://www2.chemistry.msu.edu/faculty/reusch/VirtTxtJml/Spectrpy /UV-Vis/spectrum.htm

[30] A. Kojima, K. Teshima, Y. Shirai and T. Miyasaka, Photosensor detection of OIHPs using UV-Vis spectroscopy. J. Am. Chem. Soc., 2009, 131, 6050–6051

[31] X-ray reflection in accordance with Bragg's Law, http://serc.carleton.edu; 2012

[32] C.C. Chang, C.S. Tang, 2D growth study using X-Ray Diffraction. *Journal of Applied Physics*, 87 (2000) 3931-3936.

[33] R.E. Dinnebier, S.J.L. Billinge, Principles of Powder Diffraction: Theory and Practice, 2008, The Royal Society of Chemistry, UK.

[34] Richard Tilley. "Crystals and crystal structures", Chapter 6 "Diffraction and crystal structures", John Wiley & Sons Ltd, 2006.

[35] Schlenk Line : https://www.asynt.com/product/schlenk-lines/

[36] Wan Deng, Zun-Yi Deng, Jiawei He, Mingzi Wang, Zi-Xuan Chen, Su-Huai Wei , and Hong-Jian . Synthesis of Cs2AgSbCl6 and improved optoelectronic properties of Cs2AgSbCl6. Applied Physics Letters, 111, 151602 (2017)

[37] Manoj K. Jana, Svenja M. Janke, David J. Dirkes, Seyitliyev Dovletgeldi, Chi Liu, Xixi Qin, Kenan Gundogdu, Wei You, Volker Blum and David B. Mitzi, "Direct-Bandgap 2D Silver–Bismuth Iodide Double Perovskite: The Structure-Directing Influence of an Oligothiophene Spacer Cation", *J. Am. Chem. Soc.* 2019, 141, 19, 7955–7964